

A new structure determination of the magnesium phosphate mineral struvite (MgNH₄PO₄ · 6H₂O) at 100 K

Rebecca Volkmann^{1,2} (rebeccav@gfz-potsdam.de), Marie Münchhalfen³ (marie.muenchhalfen@ruhr-unibochum.de), Liane G. Benning^{1,2} (liane.g.benning@gfz-potsdam.de)

¹German Research Centre for Geosciences GFZ, Potsdam, 14472, Germany

²Freie Universität Berlin, 14195 Berlin, Germany

³Ruhr-Universität Bochum, 44801 Bochum, Germany

Correspondence to: Rebecca Volkmann (rebeccav@gfz-potsdam.de)

A new structure determination of the magnesium phosphate mineral struvite ($\text{MgNH}_4\text{PO}_4 \cdot 6\text{H}_2\text{O}$) at 100 K

Rebecca Volkmann^{1,2}, Marie Münchhalfen³, Liane G. Benning^{1,2}

¹German Research Centre for Geosciences GFZ, Potsdam, 14472, Germany

²Freie Universität Berlin, 14195 Berlin, Germany

³Ruhr-Universität Bochum, 44801 Bochum, Germany

Correspondence to: Rebecca Volkmann (rebeccav@gfz-potsdam.de)

Abstract

The magnesium phosphate mineral struvite ($\text{MgNH}_4\text{PO}_4 \cdot 6\text{H}_2\text{O}$) is of interest for the recovery of phosphorus from wastewaters and for use as a fertilizer in agriculture, yet its structure is still debated. The structure of synthetic single crystals of struvite was characterized through refinement of a single-crystal X-ray diffraction pattern acquired at 100 K with the positions of all hydrogen atoms being identified through subsequent difference Fourier analyses. We show that the ionic interactions between the Mg^{2+} and NH_4^+ cations and the phosphate anions are reinforced by a three-dimensional network of hydrogen bonds of moderate strength. In contrast to the previously published struvite structure determined at room temperature, the ammonium groups do not rotate but are locked by three hydrogen bonds to neighboring oxygen atoms. It is likely that the rotation of the NH_4^+ groups that occurs when approaching room temperature plays an essential role in the known decomposition of struvite to newberryite ($\text{MgHPO}_4 \cdot 3\text{H}_2\text{O}$), ammonia, and water.

Chemical Context

The magnesium phosphate mineral struvite occurs naturally in phosphorous-rich soils (Teschemacher, 1846), in kidney stones comprising a sub-group called infection stones (Das *et al.*, 2017), and as a common precipitate in wastewater pipelines. As phosphorous is a limited but crucial resource, research on the formation, stability and transformation of phosphate minerals such as struvite aims to provide new insights into rates and mechanisms for phosphorous recovery from wastewaters and the use of such minerals as slow-release fertilizers in agriculture (Azam *et al.*, 2019). The crystal structure of struvite has been determined at room temperature (Ferraris *et al.*, 1986; Abbona *et al.*, 1984; Whitaker & Jefferey, 1970a). However, struvite is unstable but information about both its formation and stability is lacking. Under atmospheric conditions, struvite gradually decomposes into newberryite even at room temperature (Sutor, 1968; Whitaker, 1968), releasing ammonia and water, while at higher temperatures (e.g., 90 °C) struvite decomposes and transforms to an amorphous high surface area material (Hövelmann *et al.*, 2019). In order to determine what controls the stability and induces the transformation of struvite at ambient conditions, we characterized crystals synthesized in an aqueous solution, and their crystal structure was determined with X-ray diffraction carried out at 100 K.

Structural Commentary

The crystal structure of struvite at 100 K was solved in the polar orthorhombic space group $\text{Pmn}2_1$ (for details, see Tab. 1). The positions of all hydrogen atoms were determined by difference Fourier analysis and refined using individual isotropic displacement parameters. The structure consists of octahedral $[\text{Mg}(\text{H}_2\text{O})_6]^{2+}$ complexes and tetrahedral PO_4^{3-} and NH_4^+ groups (Fig. 1), which are linked by ionic interactions reinforced by a three-dimensional network of hydrogen bonds. The Mg–O bond lengths vary between 2.048 Å and 2.107 Å, the O–Mg–O-angles deviate by up to about 5 ° from those of an ideal octahedron (Tab. 2). All water molecules of the $[\text{Mg}(\text{H}_2\text{O})_6]^{2+}$ complex are involved in strong hydrogen bonds to oxygen atoms of neighbored phosphate groups, which in turn are characterized by donor-acceptor distances of on average 2.65 Å (Tab. 3). The tetrahedral PO_4^{3-} group is only slightly distorted with mean P–O bond lengths and P–O–P angles of ~ 1.54 Å and ~ 109.47 °, respectively (Tab. 2). Charge compensation is achieved by NH_4^+

molecules located in the cavities between the $[\text{Mg}(\text{H}_2\text{O})_6]^{2+}$ and PO_4^{3-} groups (Fig. 1) and with the ammonium group connected to the phosphate group and the $[\text{Mg}(\text{H}_2\text{O})_6]^{2+}$ groups by hydrogen bonds of the type N–H1C···O6 and N–H1D···O2, respectively (Tab. 3 and Fig. 3). The latter hydrogen bond occurs twice due to symmetry. Therefore, the ammonium group is fixed in its position and does not rotate at 100 K.

Database Survey

The crystal structure of struvite was first studied by Whitaker & Jefferey (1970a) at ambient temperatures using double-film equi-inclination Weissenberg photographic X-ray diffraction, that at that time did not allow the determination of the positions of all H atoms. However, they presented evidence for the rotation of the ammonium group around a single bond (Whitaker & Jefferey, 1970b). Later, Abbona *et al.* (1984) employing X-ray diffraction and Ferraris *et al.* (1986) using neutron diffraction improved the knowledge of the arrangement of hydrogen atoms in struvite, and suggested that at room temperature the ammonium group is ordered and linked by one single and several polyfurcated N···O bonds.

Regarding the positions of non-hydrogen atoms and taking into account thermal expansion effects, our results at 100 K agree well with literature data at room temperature. The determined hydrogen bond lengths are in good agreement with Abbona *et al.* (1984), but are ~ 0.1 Å shorter than the bond lengths reported by Ferraris *et al.* (1986). The temperature factors for water hydrogen atoms are improved by ~ 0.38 Å², compared to Abbona *et al.* (1984). Especially the thermal parameters of the hydrogen atoms of the ammonium groups atoms are reduced by up to ~ 0.04 Å² compared to the U_{iso} values derived by Ferraris *et al.* (1986). Furthermore, Ferraris *et al.* (1986) also mention the connection of the NH_4^+ group by only one single hydrogen bond and describe the other N···O bonds as polyfurcated. We could not confirm the Ferraris *et al.* (1986) arrangement by our structure solution but our description of the hydrogen bonding network agrees well with Abbona *et al.* (1984).

In summary, we show that the locking of the NH_4^+ group by several H–bonds at 100 K gives evidence to the increased stability of struvite at temperatures below 273 K. With increasing temperature, the weakening of the N–H1D···O2 bond, likely initiates a possible bouncing rotation of the ammonium group that leads eventually to the decomposition of struvite.

Synthesis and Crystallization

Struvite was synthesized using a counterdiffusion crystallization method according to Hövelmann *et al.* (2019): 1.0 M solutions of $(\text{NH}_4)_2\text{HPO}_4$ and $\text{MgCl}_2 \cdot 6\text{H}_2\text{O}$ were filled separately into 100 ml glass beakers up to their rims. They were placed at opposite sides of a 6 l plastic box. This box was then filled with de-ionized Milli-Q water until the two beakers were fully immersed. Finally, the box was closed with a lid to avoid evaporation. Crystals started to form at the bottom of the plastic container as well as at the outlets of the two beakers after a few days and had been left to grow for about two weeks until they reached sizes of several millimeters. Thereafter, the crystals were removed from the solution, rinsed with Milli-Q water and dried in air at 295 K (22 °C) for 2 h until stored in plastic membrane boxes in a fridge at 273 K (0 °C).

Refinement

Crystal data, data collection, and structure refinement details are summarized in Tab. 1. All non-hydrogen atoms were refined anisotropically. Hydrogen atom positions were identified by difference Fourier analysis and refined using the riding model. N···H and O···H bond distances were refined using similarity restraints.

Table 1 Experimental details

Crystal data	strv_unaltered
Chemical formula	$\text{H}_{12}\text{MgO}_6\cdot\text{O}_4\text{P}\cdot\text{H}_4\text{N}$
M_r	245.42
Crystal system, space group	Orthorhombic, $Pmn2_1$
Temperature (K)	100
a, b, c (Å)	6.9484 (2), 6.1038 (2), 11.1930 (5)
V (Å ³)	474.71 (3)
Z	2
Radiation type	Mo $K\alpha$
μ (mm ⁻¹)	0.39
Crystal size (mm)	0.22 × 0.14 × 0.08
Data collection	
Diffractometer	XtaLAB Synergy, Dualflex, Pilatus 300K
Absorption correction	Gaussian
	<i>CrysAlis PRO</i> 1.171.41.119a (Rigaku Oxford Diffraction, 2021) Numerical absorption correction based on Gaussian integration over a multifaceted crystal model. Empirical absorption correction using spherical harmonics as implemented in SCALE3 ABSPACK scaling algorithm
T_{\min}, T_{\max}	0.609, 1.000
No. of measured, independent and observed [$I > 2\sigma(I)$] reflections	13014, 2424, 2241
R_{int}	0.047
$(\sin \theta/\lambda)_{\max}$ (Å ⁻¹)	0.833
Refinement	
$R[F^2 > 2\sigma(F^2)],$ $wR(F^2), S$	0.028, 0.066, 1.02
No. of reflections	2424
No. of parameters	106
No. of restraints	7

H-atom treatment	All H-atom parameters refined
$\Delta\rho_{\text{max}}$, $\Delta\rho_{\text{min}}$ (e Å ⁻³)	0.45, -0.28
Absolute structure	Flack x determined using 984 quotients $[(I+)-(I-)]/[(I+)+(I-)]$ (Parsons, Flack and Wagner, Acta Cryst. B69 (2013) 249-259).
Absolute structure parameter	-0.04 (5)

Table 2 Bond lengths and angles of non-hydrogen bonds (Å, °)

Atoms	Length	Atoms	Angle
P1–O5	1.5425(15)	O5–P1–O6	109.67(9)
P1–O6	1.5478(16)	O7–P1–O5	108.68(5)
P1–O7 ¹	1.5413(11)	O7–P1–O5	108.67(5)
P1–O7	1.5413(11)	O7–P1–O6	109.49(6)
		O7–P1–O6	109.49(6)
		O7–P1–O7 ¹	110.82(8)
Mg1–O1 ²	2.0477(14)	O1–Mg1–O1 ²	89.36(8)
Mg1–O1	2.0477(14)	O1 ² –Mg1–O2 ²	87.70(5)
Mg1–O2	2.0744(12)	O1–Mg1–O2 ²	176.62(6)
Mg1–O2 ²	2.0744(12)	O1–Mg1–O2	87.70(5)
Mg1–O3	2.1070(19)	O1 ² –Mg1–O2	176.62(7)
Mg1–O4	2.1028(19)	O1 ² –Mg1–O3	89.34(6)
		O1–Mg1–O3	89.34(6)
		O1–Mg1–O4	90.36(6)
		O1 ² –Mg1–O4	90.36(6)
		O2–Mg1–O2 ²	95.19(7)
		O2–Mg1–O3	88.96(5)
		O2 ² –Mg1–O3	88.96(5)
		O2–Mg1–O4	91.32(5)
		O4–Mg1–O3	91.32(5)
			179.59(9)

¹1-x,+y,+z; ²-x,+y,+z

Table 3 Hydrogen-bond geometry (\AA , $^\circ$)

$D-\text{H}\cdots A$	$D-\text{H}$	$\text{H}\cdots A$	$D\cdots A$	$D-\text{H}\cdots A$
O4—H4A···O5 ⁱ	0.83 (3)	1.85 (3)	2.672 (2)	178 (4)
O1—H1A···O7 ⁱⁱ	0.83 (2)	1.84 (2)	2.6477 (14)	164 (3)
O1—H1B···O5	0.81 (2)	1.82 (2)	2.6225 (15)	170 (3)
O2—H2A···O6	0.83 (2)	1.88 (2)	2.6936 (16)	166 (3)
O2—H2B···O7 ⁱⁱⁱ	0.84 (2)	1.81 (3)	2.6310 (17)	168 (3)
O3—H3···O7	0.86 (3)	1.79 (3)	2.6496 (14)	175 (3)
N1—H1C···O6	0.93 (2)	1.85 (2)	2.785 (3)	180 (3)
N1—H1D···O2 ^{iv}	0.91 (2)	2.11 (2)	2.971 (2)	158 (2)
N1—H1E···O1 ⁱⁱⁱ	0.92 (3)	2.55 (4)	3.150 (2)	123 (3)
N1—H1E···O1 ^v	0.92 (3)	2.55 (4)	3.150 (2)	123 (3)

ⁱ1/2-x,-y,1/2+z; ⁱⁱ+x,-1+y,+z; ⁱⁱⁱ1/2-x,1-y,1/2+z; ^{iv}1-x,1+y,+z; ^v1/2+x,1-y,1/2+z

Table 4 Fractional Atomic Coordinates ($\times 10^4$) and Equivalent Isotropic Displacement Parameters ($\text{\AA}^2 \times 10^3$). U_{eq} is defined as 1/3 of the trace of the orthogonalised U_{ij} .

Atom	x	y	z	U_{eq}
P1	5000	4993.9(8)	3945.9(5)	6.41(9)
O5	5000	2679(2)	3393.3(15)	9.4(2)
O6	5000	4818(2)	5325.4(15)	9.5(3)
O7	3174.0(15)	6209.3(16)	3531.3(11)	9.42(18)
Mg1	0	1286.9(12)	5223.1(7)	7.78(13)
O1	2072.2(16)	250.8(17)	4051.5(14)	13.1(2)
O2	2204.4(16)	2370.5(19)	6324.4(10)	11.0(2)
O3	0	4372(3)	4378.2(17)	15.0(3)
O4	0	-1803(3)	6054.2(16)	15.0(3)
N1	5000	8724(3)	6611.2(19)	13.9(3)

Table 5 Anisotropic thermal displacement parameters (\AA^2) ($\times 10^4$). The anisotropic displacement factor exponent takes the form: $-2\pi^2[h^2a^{*2} \times U_{11} + \dots + 2hka^* \times b^* \times U_{12}]$.

Atom	U_{11}	U_{22}	U_{33}	U_{23}	U_{13}	U_{12}
P1	6.25(17)	6.04(17)	6.94(19)	0.08(16)	0	0
O5	10.7(6)	6.7(5)	10.6(6)	-1.9(5)	0	0
O6	10.9(6)	10.7(6)	7.0(6)	0.2(5)	0	0
O7	7.3(4)	9.7(4)	11.3(5)	1.0(4)	-0.8(3)	1.5(3)
Mg1	7.6(3)	7.6(3)	8.2(3)	-0.1(2)	0	0
O1	11.4(4)	9.9(4)	18.1(6)	-2.8(5)	5.4(4)	-0.7(3)
O2	10.6(5)	13.1(5)	9.4(5)	-0.7(4)	0.1(4)	-2.1(3)
O3	7.9(6)	13.6(7)	23.4(9)	7.6(6)	0	0
O4	25.5(9)	9.0(7)	10.7(7)	1.3(5)	0	0
N1	14.0(8)	13.1(8)	14.7(9)	-2.3(6)	0	0

Figures

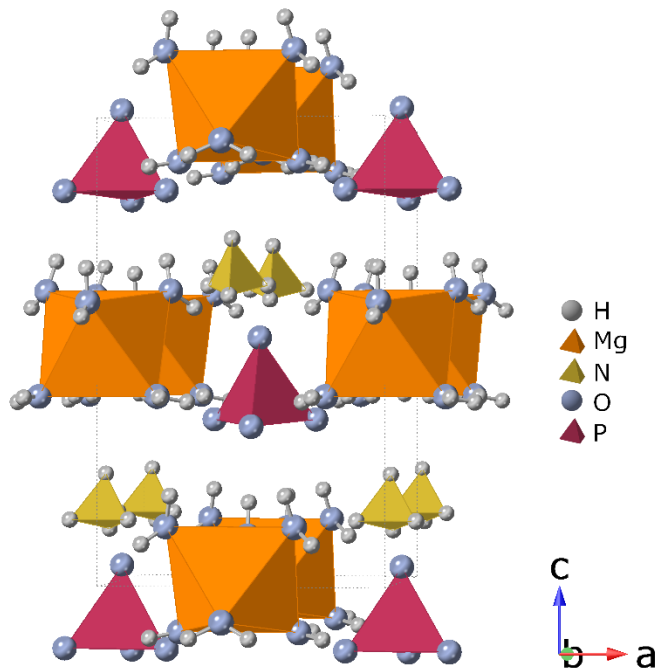


Fig. 1: Polyhedral model of the struvite crystal structure approximately along b . Figure created with CrystalMaker (Palmer, 2014).

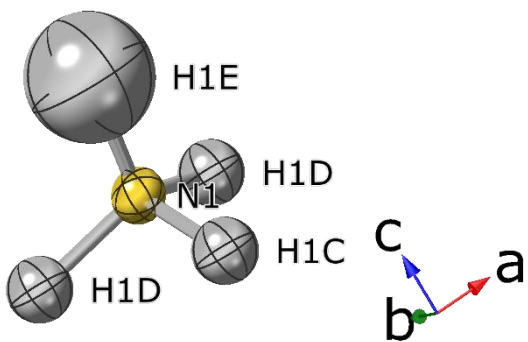
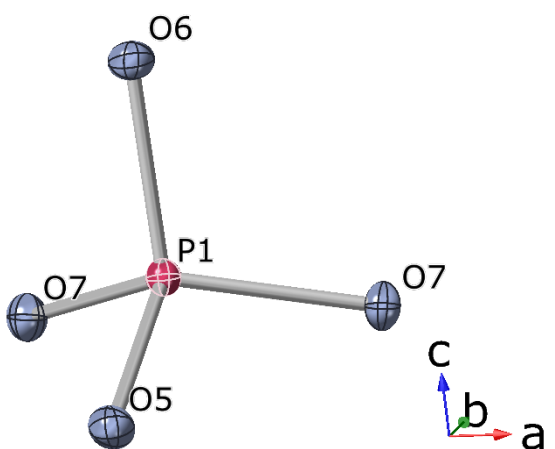
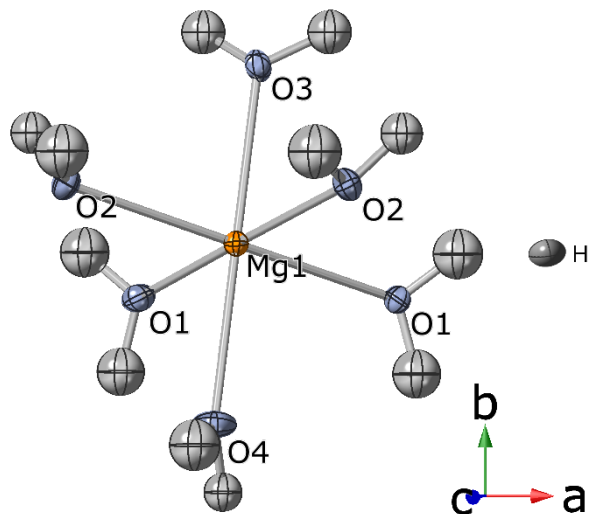


Fig. 2: Ellipsoidal models and coordination environment of single structural components of the struvite structure at 100 K. Ellipsoids are modelled with a 50 % probability. Figure created with CrystalMaker (Palmer, 2014).

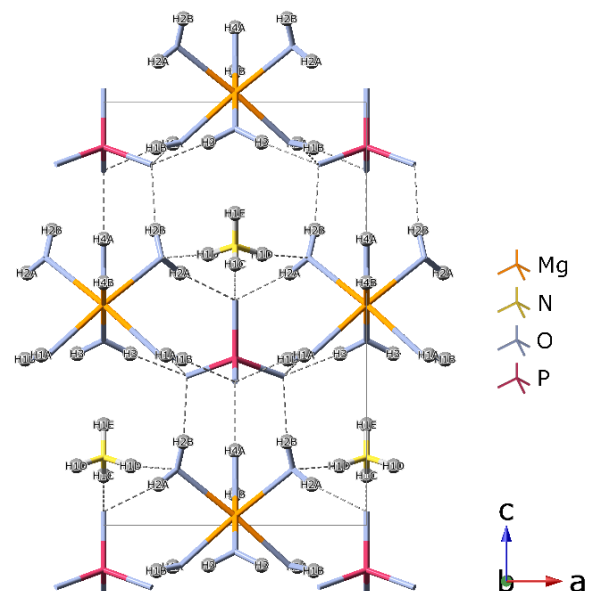
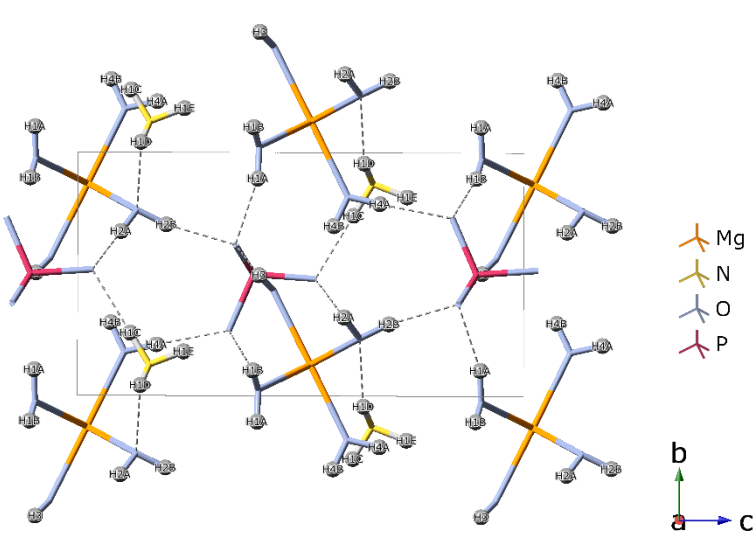


Fig. 3: Network of hydrogen bonds in struvite. Projection of structure at 100 K along **a** (left) and along **b** (right). Figure created with CrystalMaker (Palmer, 2014).

References

- Abbona, F., Calleri, M., Ivaldi, G. (1984). *Acta Cryst.* **B40**, 223–227.
- Azam, H. M., Alam, S. T., Hasan, M., Yameogo, D. D. S., Kannan, A. D.; Rahman, A., Kwon, M. J., et al. (2019). *Environ. Sci. Pollut. Res.* **26**:20, 20183–20207.
- CrysAlis PRO* 1.171.41.119a (Rigaku Oxford Diffraction, 2021)
- Das, P., Gupta, G., Velu, V., Awasthi, R., Dua, K., Malipeddi, H. (2017). *Biomed. & pharmacother.* **96**, 361–370.
- Dolomanov, O. V., Bourhis, L. J., Gildea, R. J., Howard, J. A. K. & Puschmann, H. (2009). *J. Appl. Cryst.* **42**, 339–341.
- Ferraris, G., Fuess, H. & Joswig, W. (1986). *Acta Cryst.* **B42**, 253–258.
- Hövelmann, J., Stawski, T. M., Besselink, R., Freeman, H. M., Dietmann, K. M., Mayanna, S., Pauw, B. R. & Benning, L. G. (2019). *Nanoscale* **11**, 6939–6951.
- Jeffrey, G.A (1997). *An Introduction to hydrogen bonding*, p. 12. New York: Oxford University Press.
- Palmer, D. C. (2014). *CrystalMaker*. CrystalMaker Software Ltd, Begbroke, Oxfordshire, England.
- Sheldrick, G. M. (2015). *Acta Cryst.* **A71**, 3–8.
- Sheldrick, G. M. (2015). *Acta Cryst.* **C71**, 3–8.
- Sutor, D.J. (1968). *Nature*. **218**, 295.
- Teschemacher, E. F. (1846). *Lond. Edinb. Dublin philos. mag. j. sci.* **28**, 546–550.
- Whitaker, A. (1968). *Mineral. Mag. J. Mineral. Soc.* **36**, 820-824.
- Whitaker, A. & Jeffery, J. W. (1970a). *Acta Cryst.* **B26**, 1429–1440.
- Whitaker, A. & Jeffery, J. W. (1970b). *Acta Cryst.* **B26**, 1440–1444.